

**Isoscalar Giant Resonance Strengths in ^{32}S
and possible excitations of superdeformed and $^{28}\text{Si} + \alpha$ cluster
bandheads**

M. Itoh^{1*}, S. Kishi², H. Sakaguchi², H. Akimune³, M. Fujiwara¹, U. Garg⁴,
K. Hara¹, H. Hashimoto¹, J. Hoffman⁴, T. Kawabata⁵, K. Kawase¹, T. Murakami²,
K. Nakanishi¹, B. K. Nayak⁴, S. Terashima², M. Uchida¹, Y. Yasuda², M. Yosoi²

¹ *Research Center for Nuclear Physics (RCNP),*

Osaka University, Osaka 567-0047, Japan

² *Department of Physics,*

Kyoto University, Kyoto 606-8502, Japan

³ *Department of Physics,*

Konan University,

Hyogo 658-8501, Japan

⁴ *Physics Department,*

University of Notre Dame,

Notre Dame, IN 46556, USA

⁵ *Center for Nuclear Study,*

University of Tokyo, Wako,

Saitama 351-0198, Japan

(Dated: February 20, 2018)

* Present address : Cyclotron and Radioisotope Center, Tohoku University, Sendai, Miyagi 980-8578, Japan

Abstract

Isoscalar giant resonances and low spin states in ^{32}S have been measured with inelastic α scattering at extremely forward angles including zero degrees at $E_\alpha = 386$ MeV. By applying the multipole decomposition analysis, various excited states are classified according to their spin and parities (J^π), and are discussed in relation to the super deformed and $^{28}\text{Si} + \alpha$ cluster bands.

PACS numbers: 21.10.Re, 24.50.+g, 25.55.Ci, 27.30.+t

I. INTRODUCTION

Giant resonances of nuclei are a clear manifestation of the strong collective excitation modes in many-body quantum systems. Detailed experimental and theoretical studies have been devoted to find out all possible giant resonances with various multipole transitions [1]. Inelastic α scattering has been used as the most suitable tool to extract isoscalar multipole strengths. Since α particle has $S = 0$ and $T = 0$ and the first excited state is as high as 20.2 MeV, only isoscalar natural parity transitions are strongly excited, (an exception is the weak Coulomb excitation of the isovector giant dipole resonance, $T = 1$ and $L = 1$). At extremely forward scattering-angles including 0° , cross sections for states with small transferred angular momenta (L) are strongly enhanced. In addition, α angular distributions at high bombarding energies are characterized by clear diffraction patterns. These characteristic features allow us to reliably determine the multipole transition strengths. In fact, by means of the multipole decomposition analysis (MDA), many isoscalar giant resonances have been successfully determined, and their excitation strengths have been extracted in recent years by the RCNP and the Texas A & M groups [2–13].

The giant resonances in ^{24}Mg , ^{28}Si and ^{40}Ca have been already studied by both groups. Among these light nuclei, of special interest are the giant resonances in ^{32}S with proton and neutron numbers of 16. Various theoretical models such as mean-field approaches, the shell model, and cluster-structure and molecular-resonance points of view, have predicted that there must exist well-developed superdeformed (SD) bands at high excitation energies in ^{32}S . This interesting prediction is made on basis of the concept that when the ^{32}S nucleus attains a superdeformed shape, with the ratio 2:1 for the long and short axes, nucleon number 16 becomes a magic number and the advent of a stable SD band is expected at high excitation energies [14–16]. Also, ^{32}S is a key nucleus to understand the relation between the SD structure in heavy nuclei and the cluster structure in light nuclei. The SD bands in many light nuclei, such as $^{36,38}\text{Ar}$, ^{40}Ca , and ^{56}Ni [17–20] have been discovered in the last decade. Therefore, many experiments have been performed [21–23] in order to search for the SD band in ^{32}S . However, no clear evidence for the SD band in ^{32}S has so far been reported.

In the present work, we report the results on the $^{32}\text{S}(\alpha, \alpha')$ experiment at $E_\alpha = 386$ MeV. We find candidate states that might constitute the SD and $^{28}\text{Si} + \alpha$ cluster bands in ^{32}S .

II. EXPERIMENT

The experiment was performed at the Ring Cyclotron Facility of Research Center for Nuclear Physics (RCNP), Osaka University. The details of the experimental setup and procedure are described in Ref. [3]. Here, we present the brief outline of the experiment and procedures specific to the present measurement.

Inelastic scattering of 386 MeV α particles from ^{32}S has been measured at forward angles ($\theta_{lab} = 0^\circ \sim 10.5^\circ$). In order to identify low- J^π values of complicated overlapping states, background-free measurements in inelastic α scattering at forward angles including 0° were greatly helpful. We used two self-supporting natural sulfur foils with thicknesses of 14.3 mg/cm² for 0° and of 15.6 mg/cm² for finite angles. The sulfur target was prepared in the following procedure [24]. At first, the natural sulfur powder (the abundance of ^{32}S is 95.02%) was melted at the temperature of 112.8°C. The liquid sulfur was solidified between a couple of the Teflon sheets with a well defined thickness. The target was kept cool during the measurement with liquid nitrogen by using the target cooling system described in Ref. [25] to avoid subliming the sulfur.

Inelastically scattered α particles were momentum analyzed in the high resolution spectrometer, GRAND RAIDEN [26], and detected in the focal-plane detector system consisting of two multi-wire drift-chambers and two plastic scintillators. The scattering angle at the target and the momentum of the scattered particles were determined by the ray-tracing method. The energy spectra have been obtained in the range of $5 \leq E_x \leq 52$ MeV at $\theta_{lab} = 2.5^\circ \sim 9^\circ$ and of $6 \leq E_x \leq 50$ MeV at 0° . Measurements were performed with two different energy-bite settings at each angle. In the 0° measurements, the primary beam was stopped at the just behind of the D2 magnet of GRAND RAIDEN for the high excitation energy bite and at the downstream of the focal-plane detector system for the low excitation energy bite. At forward angles from 2.5° to 5° , the beam was stopped at the location just after the Q1 magnet. At the backward angles over 6.5° , the beam was stopped in the scattering chamber of GRAND RAIDEN. The energy resolution was less than 200 keV through all the runs.

Figure 1 shows typical energy spectra at $\theta_{lab} = 0.7^\circ$ and 4.2° . In the forward angle measurements, especially at 0° , backgrounds due to the beam halo and multiple Coulomb-scattering become very large. However, we eliminated practically all the backgrounds using

the double-focus property of the ion-optics of the GRAND RAIDEN spectrometer, though the effect of the multiple Coulomb-scattering was smaller in the $^{32}\text{S}(\alpha, \alpha')$ measurement than those in heavier nuclei such as ^{208}Pb . Elastic scattering from ^{32}S was also measured at $\theta_{c.m.} = 4^\circ$ - 27° to determine the nucleon- α interaction parameters with the same incident energy.

III. ANALYSIS

The MDA has been carried out to extract multipole transition strengths from E0 to E3, by taking into account the transferred angular momentum (L) up to $L = 13$ and minimizing the chi-square per degree of freedom. $L \geq 5$ strengths were assumed to be backgrounds due to other physical processes such as quasielastic scattering in the (α, α') reaction. The cross section data were binned in 1 MeV energy intervals to reduce the fluctuation effects of the beam energy resolution. The experimentally obtained angular distributions, $\sigma^{exp}(\theta_{c.m.}, E_x)$, have been fitted by means of the least square method with a linear combination of the calculated distributions, $\sigma^{calc}(\theta_{c.m.}, E_x)$ defined by

$$\sigma^{exp}(\theta_{c.m.}, E_x) = \sum_L a_L(E_x) \sigma_L^{calc}(\theta_{c.m.}, E_x), \quad (1)$$

where $a_L(E_x)$ is the energy weighted sum rule fraction for the L component. In the DWBA calculation, a single-folded potential model was employed, with a nucleon- α interaction of the density-dependent Gaussian form, as described in Refs. [27, 28]. The nucleon- α interaction parameters are given by:

$$\begin{aligned} V(|\mathbf{r} - \mathbf{r}'|, \rho_0(r')) &= -V(1 + \beta_V \rho_0(r')^{2/3}) \exp(-|\mathbf{r} - \mathbf{r}'|^2/\alpha_V) \\ &\quad -iW(1 + \beta_W \rho_0(r')^{2/3}) \exp(-|\mathbf{r} - \mathbf{r}'|^2/\alpha_W), \end{aligned} \quad (2)$$

where the ground state density $\rho_0(r')$ was obtained using the point nucleon density unfolded from the charge density distribution [29]. The parameters V , W , $\alpha_{V,W}$, $\beta_{V,W}$ in Eq. (2) were determined by fitting the differential cross sections of elastic α -scattering measured for ^{32}S at $E_\alpha = 386$ MeV; the fit is shown in Fig. 2, and the obtained parameters are presented in Table I. The value $\beta_{V,W} = -1.9$ was adopted from Ref. [30]. The angular distribution of the 2.23 MeV 2_1^+ state was well reproduced with the known value of $\beta_2 = 0.304$ [9]. Contribution from the isovector giant dipole (IVGDR) component, arising from the Coulomb-excitation, was subtracted above the excitation energy of 10 MeV by using the gamma absorption cross

section [31]. In the $E_x > 40$ MeV region, IVGDR strength was approximated by the tail of the Breit-Wigner function to smoothly connect to the $E_x \leq 40$ MeV region.

IV. RESULTS

Figure 3 shows strength distributions for the $L = 0$ (isoscalar giant monopole resonance, E0), $L = 1$ (isoscalar giant dipole resonance, E1), $L = 2$ (isoscalar giant quadrupole resonance, E2), and $L = 3$ (high energy octupole resonance, E3) modes. Figure 4 shows typical fitting results of the MDA. In the region above $E_x = 43.5$ MeV, the sum of $L \geq 5$ components constituted dominant part of the cross section as shown at the right lower part of Fig. 4. Therefore, energy-weighted sum rule (EWSR) values, centroid energies, and r.m.s. widths for E0, E1, and E2 have been obtained by summing up from 6 to 43 MeV. Errors were estimated by changing the summing region to ± 2 MeV (6-41 MeV and 6-45 MeV).

A total of $108 \pm 7\%$ of the E0 EWSR was found. The E0 centroid energy (m1/m0) is 23.65 ± 0.60 MeV, and the rms width is 9.43 MeV. The isoscalar E1 EWSR fraction is $103 \pm 11\%$. However, the isoscalar E1 strength continues up to $E_x \sim 50$ MeV, similar to that in ^{28}Si [10, 32]. The E2 strength was identified with 143 ± 9 % of the EWSR. The E2 centroid energy is 22.42 ± 0.65 MeV, and the rms width is 9.14 MeV.

The sum of the E3 strength between 6 MeV and 50 MeV was found to correspond to only $33 \pm 7\%$ EWSR. However, the low excitation energy part between 6 and 18 MeV comprises about 3% of the EWSR which is equal to that reported in ^{28}Si . It would appear that the high energy E3 (HEOR) strength between 18 and 43 MeV could not be separated from higher multipole ($L \geq 4$) components. The centroid energy of the HEOR is 31.4 ± 0.5 MeV which is also comparable to that of ^{28}Si . Although the low excitation energy region of the E4 strength could be separated from higher multipole ($L \geq 5$) components, as described later, it was not possible to clearly identify the E4 strength above $E_x > 25$ MeV due to featureless angular distributions, as shown in Fig. 4.

Figure 5 shows the distributions for the E0, E1, E2, and E3 strengths obtained by the MDA with a small bin size of 200 keV. for $L = 0, 1, 2, 3,$ and 4 . In order to obtain excitation energies of the $0^+, 1^-, 2^+, 3^-,$ and 4^+ levels, we fitted energy spectra with a Gaussian at $0.7^\circ, 1.9^\circ, 3.3^\circ, 4.8^\circ,$ and 5.6° , respectively. The transition strengths were estimated by integrating the strength distribution corresponding to the states. It should be noted that

their absolute values are strongly affected by the DWBA calculation used in the MDA. The extracted excitation energies and strengths are listed in Table II. In the $L = 0$ strength distribution presented in Fig. 5, there were many candidates for the E0 strength at $E_x < 14$ MeV. However, since the isovector E1 cross section due to the Coulomb-force shows also a strong peak at 0° similar to the E0 strength, it could not be excluded from the E0 strength at $E_x < 14$ MeV. A possible way to look at the IVGDR contribution is to compare the (α, α') strength distributions with those obtained from (p, p') at similar energies. Such data are available from Ref. [24]. From a comparison of the 0° spectra between the (α, α') and (p, p') reactions, we identified six 0^+ states in the E0 strength distribution of (α, α') as listed in Tables II and III.

V. DISCUSSION

A. Strength distributions of the giant resonances

In light nuclei, the isoscalar giant monopole (ISGMR) strength is fragmented into the wide excitation energy region, as reviewed in Ref. [1]. In recent works on ^{24}Mg , ^{28}Si , ^{40}Ca , and ^{48}Ca [10, 12, 33–35], a large part of the E0 strength was found over $E_x \sim 20$ MeV. The E0 strength in ^{32}S was also found to be fragmented in the wide excitation energy region from 6 MeV to 43 MeV as shown in Fig. 3(a). The E0 centroid energy of $23.65^{+0.60}_{-0.66}$ MeV is comparable to the empirical expression, $E_{ISGMR} \sim 78 A^{-1/3}$, of 24.6 MeV.

As for the centroid energy of the isoscalar giant dipole resonance (ISGDR), the E1 strength continues up to $E_x \sim 50$ MeV, as described in the previous section. The empirical expression of $E_{ISGDR} \sim 133 A^{-1/3}$ found in Ref. [2] becomes 41.9 MeV. Although the E1 strength was found almost 100% in this measurement, and since the absolute value of the strength is strongly affected by the DWBA calculation used in the MDA, it implies the measurement up to the sufficiently high excitation energy region is needed to find the whole strength of the ISGDR in light nuclei such as ^{32}S .

B. Candidate for the bandhead of the SD band in ^{32}S

The 0^+ states at $E_x = 10.49$ MeV, 11.62 MeV, 11.90 MeV are candidates for the bandhead state of the SD band. The bandhead 0^+ state of the SD band in ^{32}S is predicted to appear

at $E_x = 10 \sim 12$ MeV in the HF and HFB frameworks [14, 15]. It has also been shown that this SD band is essentially identical to the Pauli allowed lowest $N = 24$ band of the $^{16}\text{O}+^{16}\text{O}$ molecular structure [16]. It is tempting, to conjecture that these 0^+ states might, indeed, be the bandhead of a SD band. Extending this conjecture, we observe 2^+ and 4^+ members of the SD band above these excitation energies.

Figure 6 shows the two-dimensional histogram of the excitation energies versus the $J(J+1)$ values. The solid lines are drawn to guide the eye. The slope of these lines corresponds to $k \equiv \hbar^2/2\mathcal{J} = 83$ keV. Although this value is larger than predicted one of 48.5 keV in Ref. [15], it is in good agreement with a simple calculation of $k = 85$ keV obtained by the assumption of point masses for a rigid $^{16}\text{O} + ^{16}\text{O}$ molecular structure with the radius, $R = 1.1 \text{ A}^{1/3}$ fm. It is also comparable to $k = 82$ keV and 69 keV of the SD bands observed in ^{36}Ar [17, 18] and ^{40}Ca [19], respectively. However, the experimental bandheads of the SD bands in ^{36}Ar and ^{40}Ca are at low excitation energies (4.33 MeV and 5.21 MeV, respectively) in comparison with $E_x = 10 \sim 12$ MeV in ^{32}S . This high excitation energy of the bandhead might be a reason why the SD band has not been observed in γ -ray spectroscopic studies so far [36].

In a macroscopic analysis of the $^{16}\text{O} + ^{16}\text{O}$ rainbow scattering, it was concluded that the low-spin 0^+ , 2^+ , 4^+ , and 6^+ states of the $N = 24$ $^{16}\text{O} + ^{16}\text{O}$ cluster band were fragmented [37] and in an elastic $^{28}\text{Si} + \alpha$ scattering experiment, many fragmented 0^+ states were observed [23]. Therefore, the 0^+ states at $E_x \sim 11$ MeV observed in the present work could be the candidates of fragmented 0^+ states.

C. $^{28}\text{Si} + \alpha$ cluster structure

The lower excitation energy 0^+ states, at 6.6 MeV and 7.9 MeV, which are near the α -decay threshold energy in ^{32}S , are discussed in relation to the bandhead of the $^{28}\text{Si} + \alpha$ cluster band in the analogy with the $^{12}\text{C} + \alpha$ cluster in ^{16}O and the $^{16}\text{O} + \alpha$ cluster in ^{20}Ne [38]. Since there are mirror configurations of the $^{12}\text{C} + \alpha$ and $^{16}\text{O} + \alpha$ clusters, these cluster structures lead the parity-doublet rotational bands. The appearance of a parity-doublet rotational band in the asymmetric intrinsic α cluster configurations is also explained by a cluster model with a deep potential [39, 40].

The dashed and dotted lines in Fig. 6 are drawn to point out members of the parity-

doublet $^{28}\text{Si} + \alpha$ cluster band in ^{32}S . The rotational constants k corresponding to the dashed and dotted lines are 234 keV and 125 keV, respectively. The gap energy between the positive and the negative bands for the dashed line is almost zero. It indicates the $^{28}\text{Si} + \alpha$ cluster structure in this band has a rigid body. The value of 234 keV is in good agreement with a simple calculation of 245 keV obtained with the assumption of point masses for a rigid $^{28}\text{Si} + \alpha$ cluster with a radius $R = 1.1 A^{1/3}$ fm for ^{28}Si , and 1.6 fm for the α -particle. However, these simple calculations of the rotational constant are just trials to explain the experimentally-observed rotational constants. More realistic theoretical calculations are highly desired for the further detailed comparison with the experimental results.

VI. SUMMARY

We have investigated the isoscalar giant resonance strengths in the doubly-closed shell nucleus ^{32}S , with a view to search for the possible superdeformed bandhead predicted in theoretical calculations. A novel technique was used to prepare an enriched ^{32}S target, and the $^{32}\text{S}(\alpha, \alpha')$ measurements were made at extremely forward angles, including 0° at $E_\alpha = 386$ MeV. The extracted E0, E1, E2, and E3 strength distributions from MDA are similar to those in nearby light nuclei. From the MDA with a 200 keV energy bin, three 0^+ states at 10.49 MeV, 11.62 MeV, and 11.90 MeV are extracted. These three 0^+ states would be candidates for the bandhead of the SD band in ^{32}S . In addition, the parity-doublet $^{28}\text{Si} + \alpha$ cluster bands have been identified. The rotational constants obtained from the level distance for the possible rotation states are in good agreement with simple calculations with the assumption of point masses for the $^{16}\text{O} + ^{16}\text{O}$ and $^{28}\text{Si} + \alpha$ cluster structures.

Acknowledgments

We would like to thank H. Matsubara and A. Tamii for providing us with the $^{32}\text{S}(\text{p}, \text{p}')$ spectrum at 0° . We would also like to thank K. Matsuyanagi and E. Ideguchi, and Odahara for fruitful discussions. We wish to thank RCNP staff for providing the high-quality α beams required for these measurements. This work was supported in part by JSPS KAKENHI Grant Number 24740139, 24540306, and the U.S. National science Foundation (Grant Nos. INT03-42942, PHY04-57120, PHY07-58100, and PHY-1068192) and by the US-Japan

- [1] M.N. Harakeh and A. van der Woude, *Giant Resonances* (Clarendon Press, Oxford, 2001).
- [2] M. Uchida *et al.*, Phys. Rev. C **69**, 051301(R) (2004).
- [3] M. Itoh *et al.*, Phys. Rev. C **68**, 064602 (2003).
- [4] B.K. Nayak *et al.*, Phys. Lett. B **637**, 43 (2006).
- [5] T. Li *et al.*, Phys. Rev. Lett. **99**, 162503 (2007).
- [6] M. Itoh *et al.*, Nucl. Phys. **A687**, 52c (2001).
- [7] M. Itoh *et al.*, Phys. Lett. B **549**, 58 (2002).
- [8] D. Patel *et al.*, Phys. Lett. B **718**, 447 (2012).
- [9] D.H. Youngblood, J.M. Moss, C.M. Rozsa, J.D. Bronson, A.D.Bacher, and D.R. Brown, Phys. Rev. C. **13**, 994 (1976).
- [10] D.H. Youngblood, Y.-W. Lui, and H.L. Clark, Phys. Rev. C **76**, 027304 (2007).
- [11] D.H. Youngblood, Y.-W. Lui, and H.L. Clark, Phys. Rev. C **65**, 034302 (2002).
- [12] D.H. Youngblood, Y.-W. Lui, and H.L. Clark, Phys. Rev. C **63**, 067301 (2001).
- [13] Y.-W. Lui, D.H. Youngblood, H.L. Clark, Y. Tokimoto, and B. John, Phys. Rev. C **73**, 014314 (2006).
- [14] M. Yamagami, K. Matsuyanagi, Nucl. Phys. **A672**, 123 (2000).
- [15] R.R. Rodriguez-Guzman, J.L. Egido, and L.M. Robledo, Phys. Rev. C **62**, 054308 (2000).
- [16] M. Kimura and H. Horiuchi, Phys. Rev. C **69**, 051304(R) (2004).
- [17] C.E. Svensson *et al.*, Phys. Rev. Lett. **85**, 2693 (2000).
- [18] C.E. Svensson *et al.*, Phys. Rev. C **63**, 061301(R) (2001).
- [19] E. Ideguchi *et al.*, Phys. Rev. Lett. **87**, 222501 (2001).
- [20] D. Rudolph *et al.*, Phys. Rev. Lett. **82**, 3763 (1999).
- [21] K. Morita *et al.*, Phys. Rev. Lett. **55**, 185 (1985).
- [22] N. Curtis *et al.*, Phys. Rev. C **53**, 1804 (1996).
- [23] T. Lönnroth *et al.*, Eur. Phys. J. A **46**, 5 (2010).
- [24] H. Matsubara, H. Sakaguchi, S. Kishi, A. Tamii, NIM B **267**, 3682 (2009).
- [25] T. Kawabata, *et al.*, NIM A **459**, 171 (2001).
- [26] M. Fujiwara *et al.*, Nucl. Instr. Meth. in Phys. Res. **A422**, 484 (1999).

- [27] G.R. Satchler and D.T. Khoa, Phys. Rev. C **55**, 285 (1997).
- [28] A. Kolomiets, O. Pochivalov, and S. Shlomo, Phys. Rev. C **61**, 034312 (2000).
- [29] H. De Vries *et al.*, At. Data Nucl. Data Tables **36**, 495 (1987).
- [30] G. Satchler, *Direct Nuclear Reactions* (Clarendon Press, Oxford, 1983).
- [31] B.S. Ishkhanov *et al.*, Moscow State Univ.Inst.of Nucl. Phys. Reports No. **2002**, 27 (2002).
- [32] P.V. Madhusudhana Rao, unpublished results.
- [33] T. Kawabata *et al.*, Prog. of Theor. Phys. Suppl. **196**, 198 (2012).
- [34] D.H. Youngblood, Y.-W. Lui, X.F. Chen, and H.L. Clark, Phys. Rev. C **80**, 064318 (2009).
- [35] Y.-W. Lui, D.H. Youngblood, S. Shlomo, X. Chen, Y. Tokimoto, Krishichayan, M. Anders, and J. Button, Phys. Rev. C **83**, 044327 (2011).
- [36] C.E. Svensson, private communication.
- [37] S. Ohkubo and K. Yamashita, Phys. Rev. C **66**, 021301(R) (2002).
- [38] H. Horiuchi, K. Ikeda, and Y. Suzuki, Suppl. of Prog. of Theor. Phys. **52**, 89 (1972).
- [39] F. Michel, S. Ohkubo, and G. Reidemeister, Suppl. Prog. Theor. Phys. **132**, 7 (1998).
- [40] S. Ohkubo and K. Yamashita, Phys. Lett. B **578**, 304 (2004).

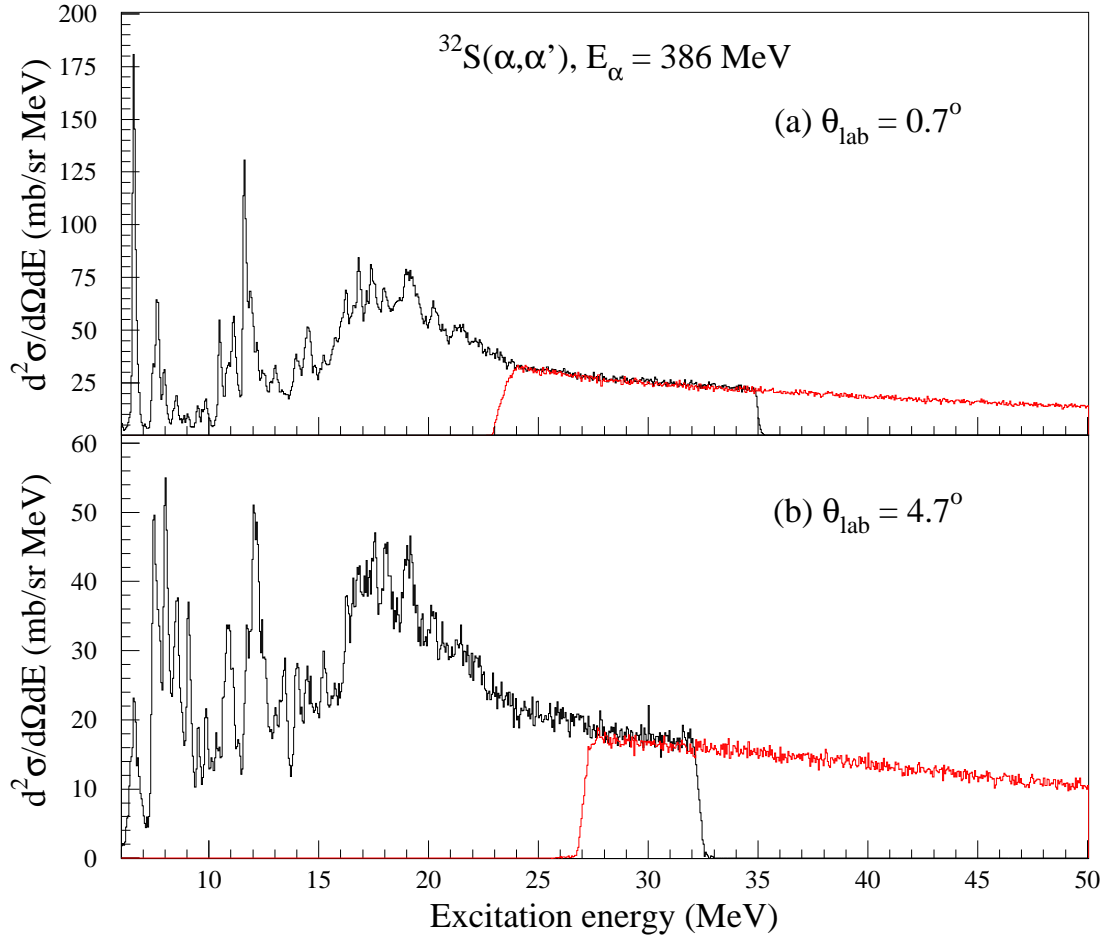


FIG. 1: (Color online) Excitation energy spectra for $^{32}\text{S}(\alpha, \alpha')$ at averaged laboratory angles of $\theta_{\text{lab}} = 0.7^\circ$ and $\theta_{\text{lab}} = 4.7^\circ$. The black line shows the energy spectrum obtained from the low excitation measurement. The red line shows that obtained from the high excitation measurement.

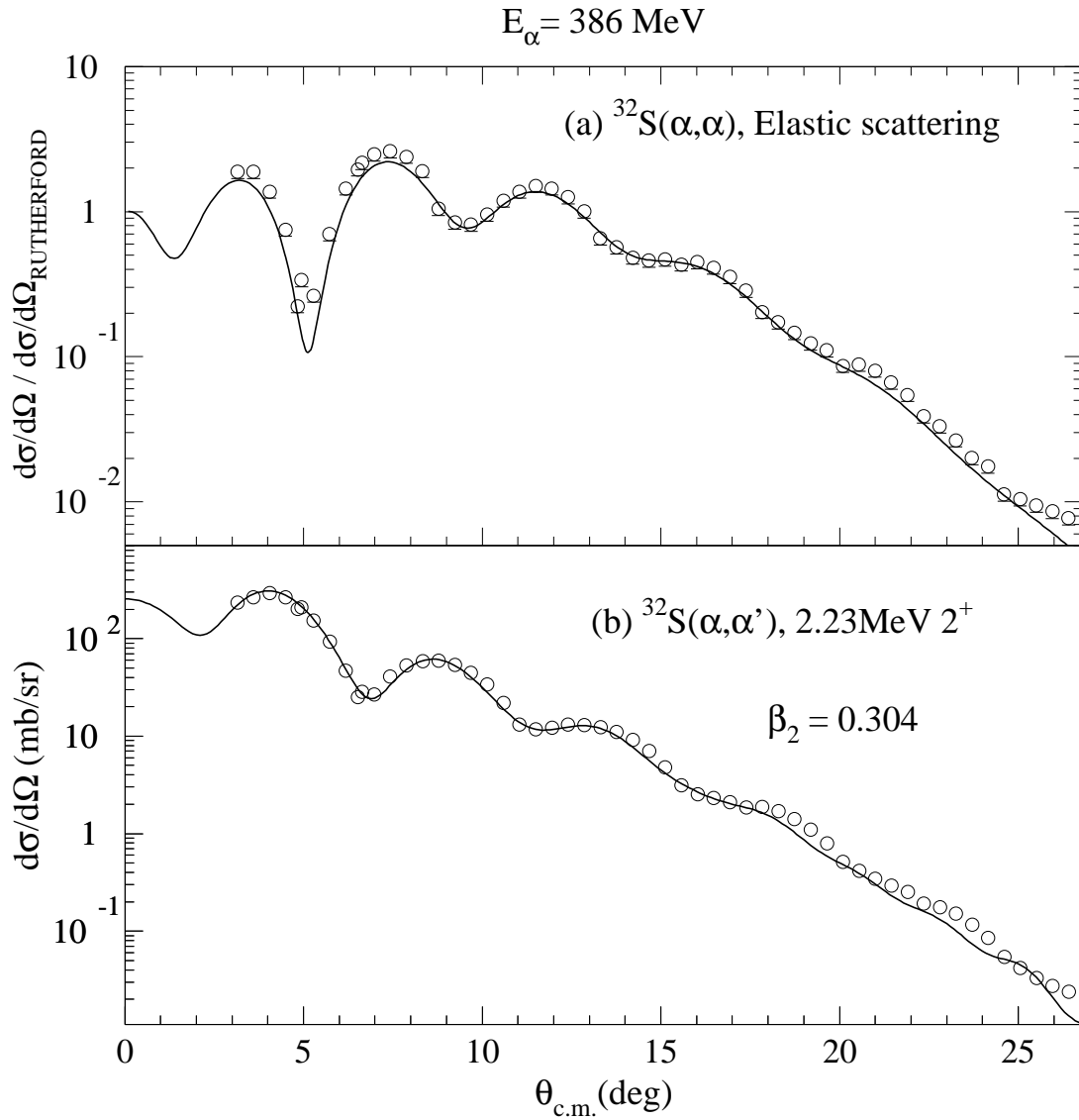


FIG. 2: (a) Angular distribution of the ratio of the differential cross section for elastic scattering to Rutherford scattering for 386 MeV α particles from ^{32}S . (b) Angular distribution of differential cross sections for the 2.23 MeV 2^+ state. In both cases, the solid lines show the results of the DWBA calculations using the single-folding model (see text).

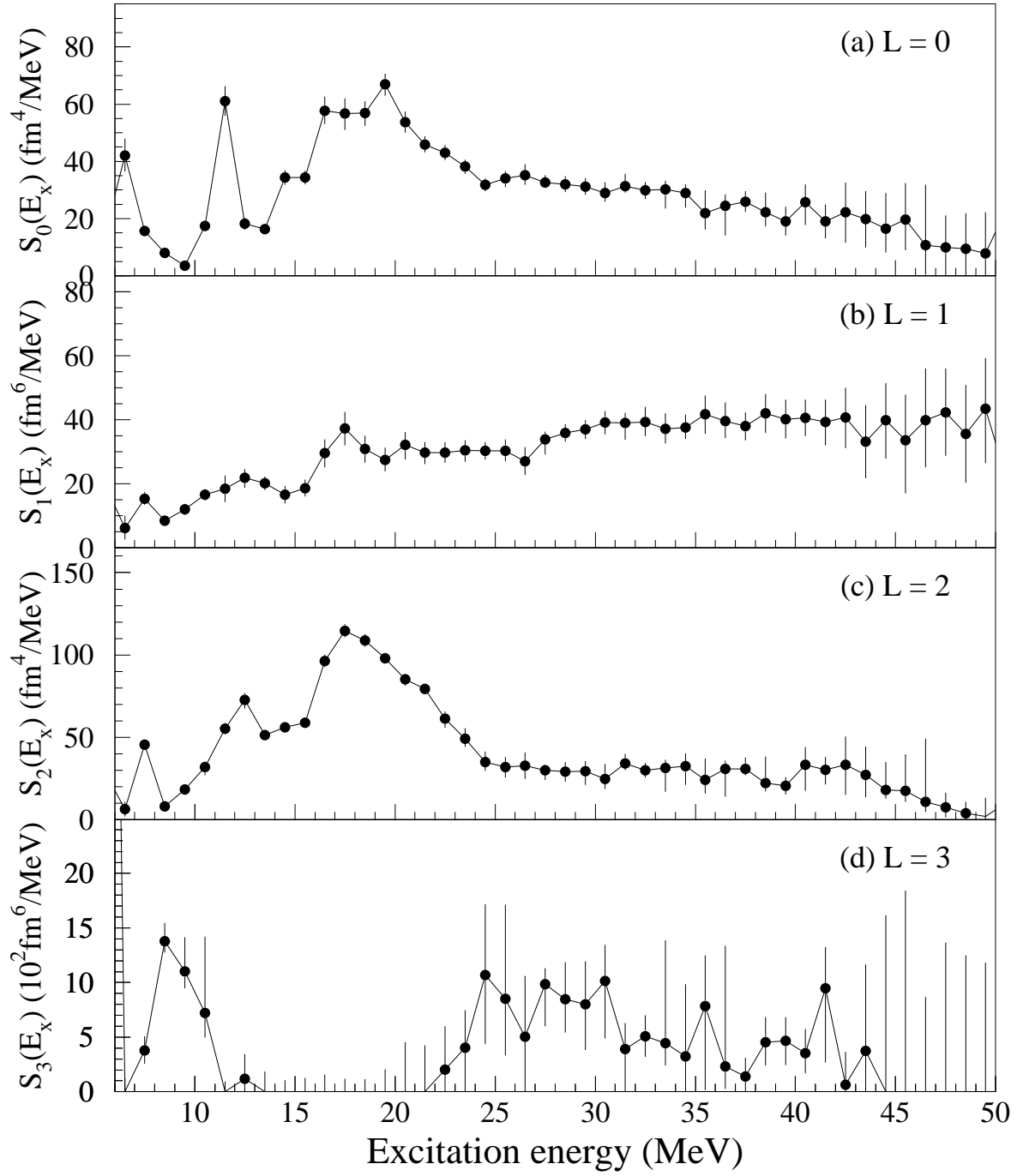


FIG. 3: Distributions with 1 MeV bins for the E0, E1, E2, and E3 strengths are presented in panels (a), (b), (c), and (d), respectively. The lines are given for the guide of eyes.

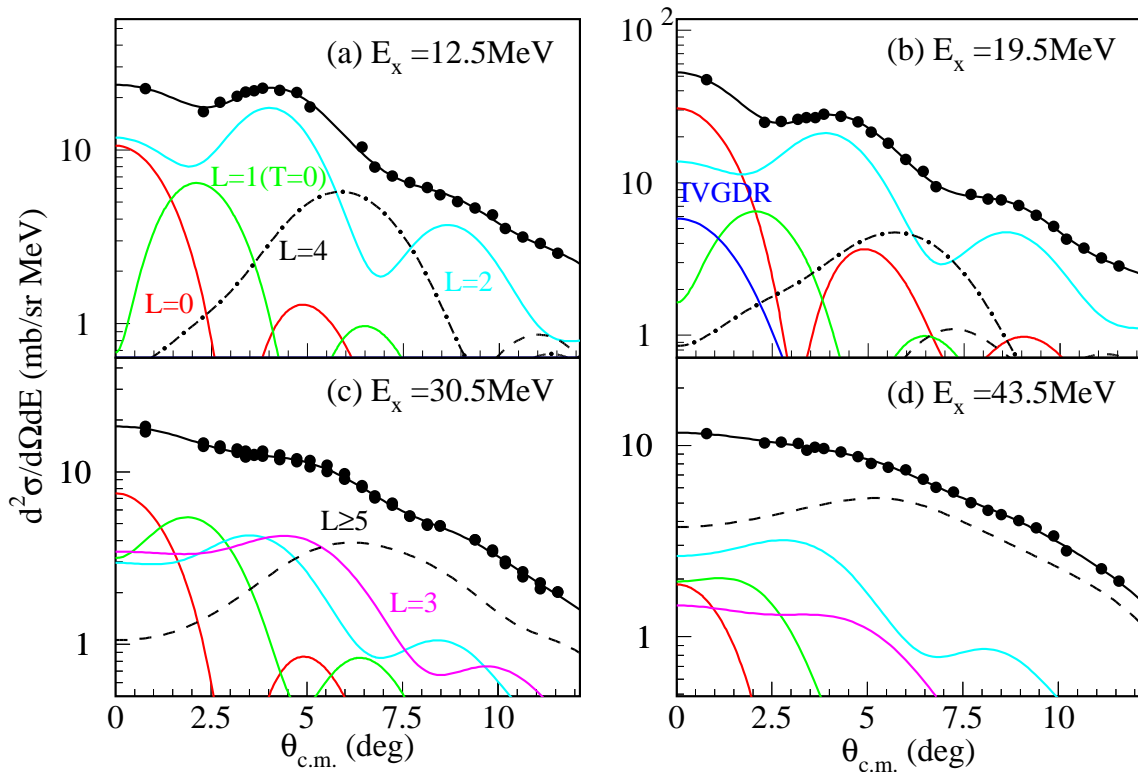


FIG. 4: (Color online) Typical angular distributions of inelastic α scattering. The line through the data shows the sum of various multipole components obtained by the MDA. Each multipole contribution is represented by the color line and the transferred angular momentum L are indicated. The blue line shows a contribution of the IVGDR estimated from the gamma absorption cross section (see text).

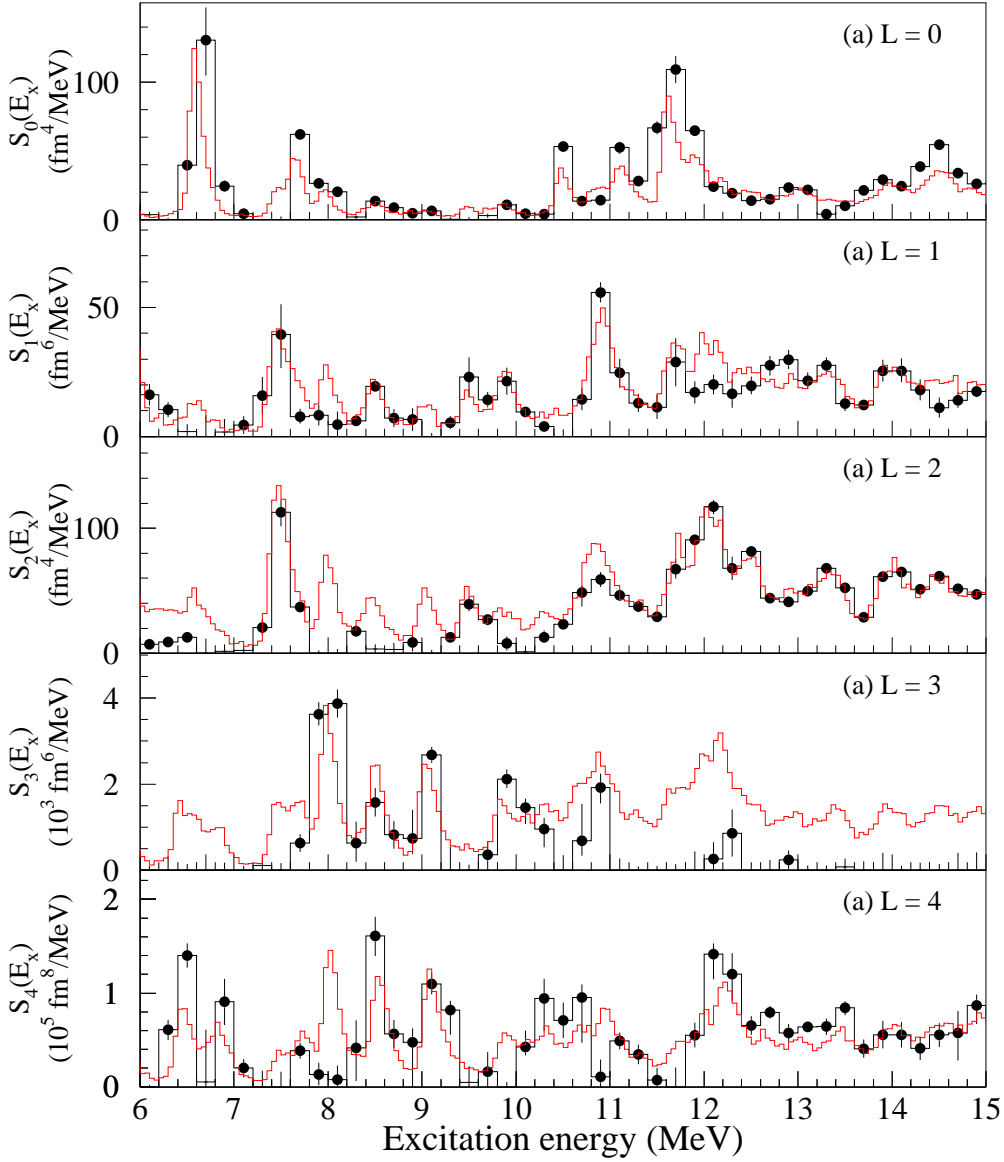


FIG. 5: (Color online) Strength distributions with a 200 keV bin for the E0, E1, E2, E3, and E4 transitions in the region from 6 MeV to 15 MeV are presented in the panels (a), (b), (c), (d), and (e), respectively. The red lines show the excitation energy spectra for the $^{32}\text{S}(\alpha, \alpha')$ reaction at (a) $\theta_{lab} = 0.7^\circ$, (b) 2.0° , (c) 3.4° , (d) 4.8° , and (e) 5.6° , respectively, scaled to fit in the figures. Some differences of peak positions between the excitation energy spectrum at $\theta_{lab} = 0.7^\circ$ and the E0 strength distribution are arising from primarily an artifact of histogramming. The differences, if any, are within the uncertainty of 0.05 MeV in peak positions.

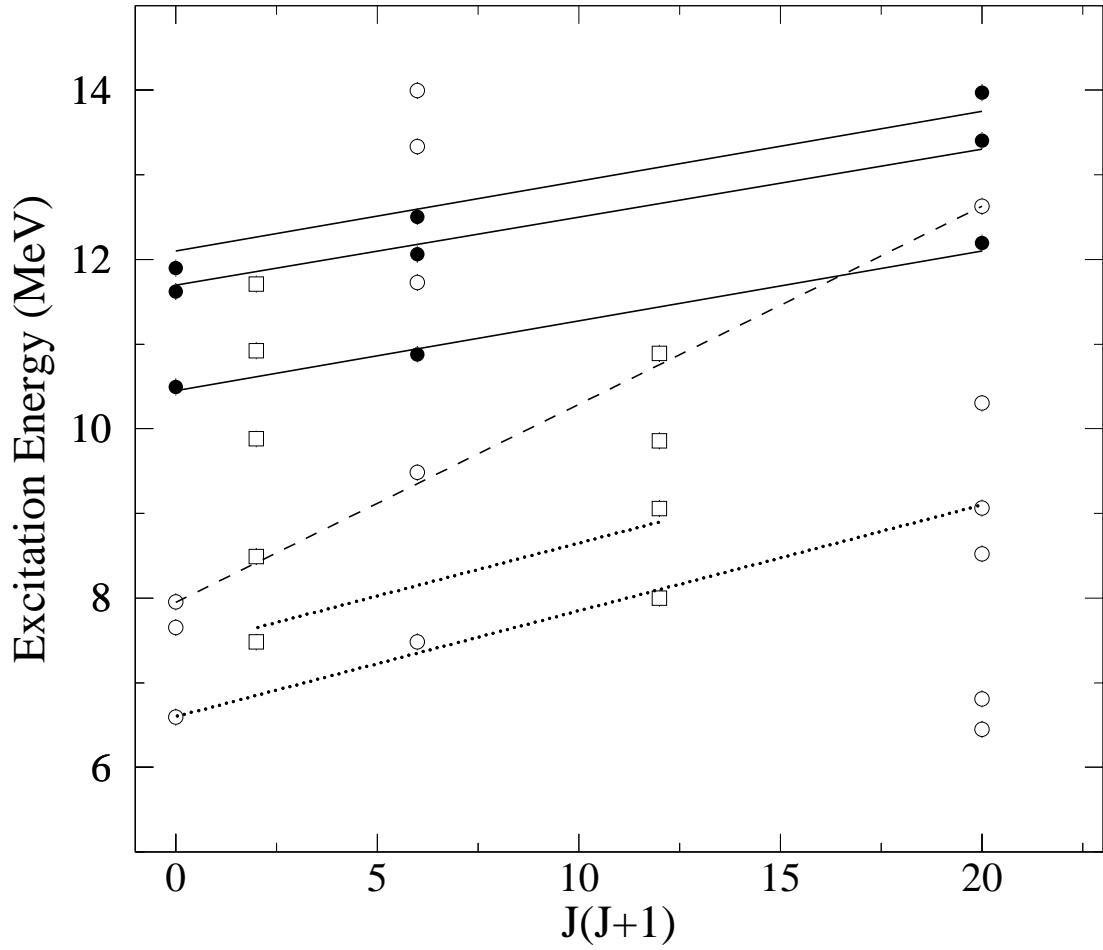


FIG. 6: Excitation energies are plotted versus $J(J+1)$ for the states obtained in this experiment. The open/closed circles show the positive parity states. The open squares show the negative parity states. Candidates for the SD band are plotted in the closed circles. The lines are displayed to guide the eyes. The rotational constants k corresponding to the solid, dashed, and dotted lines are 83 keV, 234 keV, and 125 keV, respectively.

TABLE I: The nucleon- α interaction parameters. employed in the folding-model potential used in this work. * taken from Refs. [27, 28]

	V	α_V	W	α_W	$\beta_{V,W}$
	(MeV)	(fm ²)	(MeV)	(fm ²)	(fm ²)
³² S	31.84	3.8	17.73	3.8	-1.9*

TABLE II: Observed positive parity states. Excitation energies are obtained by fitting the energy spectra with a Gaussian peak shape at 0° for the 0⁺ states, 3.3° for the 2⁺ states, and 5.6° for the 4⁺ states, respectively. Uncertainties in the excitation energies are about 0.05 MeV, which includes the fitting errors and the energy calibration errors. Each error in strengths is estimated from those of the integrated strength distributions.

Ex (MeV)	J ^{π}	Strength (fm ⁴)	Ex (MeV)	J ^{π}	Strength (fm ⁴)	Ex (MeV)	J ^{π}	Strength (10 ⁵ fm ⁸)
6.59	0 ⁺	39.8±5	7.48	2 ⁺	34.1±2.7	6.45	4 ⁺	40.2±2.2
7.65	0 ⁺	14.6±1	9.48	2 ⁺	17.3±2	6.80	4 ⁺	22.1±5.3
7.95	0 ⁺	7.2±1	10.88	2 ⁺	30.8±2.6	8.53	4 ⁺	43.5±5.2
10.49	0 ⁺	10.6±0.6	11.73	2 ⁺	19.3±1.8	9.06	4 ⁺	38.3±5
11.62	0 ⁺	29.4±2.4	12.06	2 ⁺	42.3±2.1	10.3	4 ⁺	27.4±7
11.90	0 ⁺	18.7±2.4	12.51	2 ⁺	16.3±0.7	12.19	4 ⁺	52.3±7
			13.33	2 ⁺	24.1±0.9	12.63	4 ⁺	27.4±2.3
						13.40	4 ⁺	29.8±2.4
						13.97	4 ⁺	22.2±4

TABLE III: Observed negative parity states. Excitation energies were obtained by fitting the energy spectra with a Gaussian peak shape at 1.9° for the 1^- states and 4.8° for the 3^- states, respectively. The uncertainties in excitation energies are about 0.05 MeV. Each error in strengths is obtained from those of the integrated strength distribution.

Ex (MeV)	J^π	Strength (fm^6)	Ex (MeV)	J^π	Strength (10^3 fm^6)
7.48	1^-	11 ± 5	8.0	3^-	1.5 ± 0.09
8.49	1^-	5.1 ± 0.6	9.06	3^-	0.68 ± 0.09
9.88	1^-	6.2 ± 1.2	9.86	3^-	0.42 ± 0.05
10.92	1^-	19 ± 1.4	10.89	3^-	0.52 ± 0.18
11.71	1^-	8 ± 2.1			